Infotech@Aerospace
26 - 29 September 2005, Arlington, Virginia

AIAA 2005-7009

Integrated VIS-NIR Hyperspectral / Thermal-IR Electro-Optical Payload System for a Mini-UAV

Giancarlo Rufino* and Antonio Moccia.†
University of Naples "Federico II", Napoli, I-80125, Italy

This paper presents the development of a modern electro-optical payload system for remote sensing from a mini-UAV. It is aimed at applications of natural disasters monitoring, in particular forest fires. Both the sensor and the mini-UAV platform are being developed at the Dept. of Space Science and Engineering (DISIS) of the University of Naples "Federico II." The core of the system is an integrated, multi-band sensor that includes a thermal imager and a hyperspectral sensor in VNIR band. Instrument characterization, laboratory tests, and payload architecture are discussed.

I. Introduction

Remote Sensing (RS) for monitoring and management of natural disasters is of great interest currently and increasing attention is being gained by forest fires because of their frequent occurrence and the relevance of the damage they cause. There exists several studies dealing with applications of RS to detect forest fires and to monitor them for suppression and damage mitigation [1,2,3], as well as experiments have been carried out for technology demonstration [4, 5]. Both aeronautical and satellite platforms have been considered, showing relevant performance and limitations. The latter ones, in particular, can be pointed out after considering the main issues of an ideal system for monitoring forest fires to the aim of suppression and damage mitigation [6]: ability to detect fire in its early stage and to distinguish the associated degree of danger; day-and-night operation capability; detection of fire location, extension, as well as propagation direction in relation to topography and forest resources (vegetation and fuels). Additional desirable features are long observation time ability to follow the whole duration of the event, and real-time transmission of the acquired data to users, i.e., fire management personnel, in format that allows for immediate exploitation by disaster management operators rather than RS application specialists. Because of these requirements, satellite-based systems, that showed adequate measurement performance in several experiments and that were limited only in resolution in some cases, have poor performance in terms of coverage ability [7,8]. The latter one, in fact, is restricted both in space and time because it is constrained by orbit ground track repetitivity, typically in the order of days or even weeks for medium/high resolution RS systems performing global coverage. Hence, such systems are often not available for observation at site and time of a fire event, and almost certainly they cannot follow fire evolution but just offer a single survey of it; neither platform passes over the area of interest can be adjusted for the peculiar extension and evolution of the fire under observation. On the other hand, airborne platforms offer plenty of interesting capabilities for this application: timely observation (limited only by ground base distance from the area of the event and availability of operational units), survey flight trajectory not fixed a priori but adaptable to the case and, in particular, flight altitude modifiable to satisfy resolution and instantaneous coverage requirements, flight duration that can be extended and flights that can be repeated as needed. Finally, also issues concerning distribution of acquired data is in favor of aeronautical platforms. In fact, for typical satellite RS systems, download of acquired data is not continuous but subdue to ground station links that can operate only during limited fractions of orbits. Differently, data can be transmitted from an airplane in real time by exploiting high-capacity channel radio links to a ground station or satellite communications. Then, data distribution to users community can be accomplished by means of existing networks, even the internet [6].

Recent technology progress has made possible to base the above applications on UAV platforms [4,5]. First, modern electronics, also Commercial-Off-The-Shelf (COTS) components, is characterized by high performance in spite of reduced size, mass and power consumption, so that even complex, integrated systems (RS sensors, on-board avionics and MEMS devices, computers running software logic for autonomous flight and payload operation control) are suitable for installation on board of UAVs that, typically, have limited availability of resources. Also,

* Staff scientist, Department of Space Science and Engineering, Piazzale Tecchio 80, Napoli.
† Full professor, Department of Space Science and Engineering, Piazzale Tecchio 80, Napoli, AIAA Member.

Copyright © 2005 by the American Institute of Aeronautics and Astronautics, Inc. All rights reserved.

materials progress allows now for platforms in which significant volume and mass can be devoted to payload and auxiliary subsystems. Finally, for the specific objective of a fire monitoring RS mission, unmanned vehicles offer the important feature of not endangering a human crew during risky missions as flights over areas interested by fires, permitting close surveys to achieve detailed observation that could not be attempted with a manned vehicle.

The Laboratory of Guidance, Navigation, and Control (GNC Lab) of the Department of Space Science and Engineering (DISIS) of the University of Naples "Federico II", Italy, is carrying out a series of projects dealing with the above research topics. First of all, DISIS takes part in a project of the "Centro Regionale di Competenza Analisi e Monitoraggio del Rischio Ambientale" (CRdC AMRA), a recently founded institution for coordination of regional, hi-tech laboratories carrying out activities in the field of environmental risk monitoring, and for technology transfer to practical applications. The project objective is the development of a cutting-edge RS system for compact aeronautical platforms aimed at monitoring forest fires natural disasters. In the framework of this project, DISIS is in charge of the development of an integrated multi-/hyper-spectral EO sensor [9]. It is based on four Electro-Optical (EO) instruments: a thermal camera, a 3-band multispectral camera operating in the visible (VIS) spectrum, two hyperspectral sensors operating in the Visible-Near InfraRed (VNIR) and in the Near-InfraRed (NIR) band. All of these instruments are COTS devices or they have been realized by assembling COTS components, as in he case of the hyperspectral sensors. Another activity in progress at DISIS is supported by Regione Campania, the local regional administration institution, within its plan for sustaining scientific research. It is centered on the development of the digital communication system dedicated to the RS EO payload of a compact UAV for environment monitoring applications. Also, a co-operation with the ISAFoM institute of the National Research Council (CNR) is in progress to fly the above sensors on board a two-seat, general aviation light aircraft (ERA SkyArrow) already equipped with instruments to study ground-atmosphere interaction phenomena. Finally, DISIS is developing a mini-UAV platform, with particular interest in navigation and flight control autonomous functionalities [14]. These latter activities have been supported by the Ministry for Education, University and Research (MIUR) and, in part, they have been carried out in co-operation with the Italian Aerospace Research Centre (CIRA).

In this paper, the EO payload for the mini-UAV platform and the relevant activity are described, including instrument characterization, on-board integration, and development of auxiliary on-board systems for sensor operation control. Preliminary results are presented.

II. Payload System

Several studies have been published dealing with the topic of RS for forest fires risk detection and monitoring that describe techniques for fire properties estimation by collecting the upwelling radiance in the optical bands of the spectrum, from VIS to Thermal InfraRed (ThIR) [1,2,3]. In fact, to carry out forest fires suppression and damage mitigation efficiently, besides the capability of fire detection and determination of its size and position on the ground, it is desirable to foresee fire evolution. Models have been developed that require to distinguish temperature distribution in the active fire areas and in burnt ones, as well as to ascertain the kind of vegetation in adjacent areas, if present, which could represent fuels for fire evolution. The latter issue can be effectively exploited also at the stage of prevention by mapping fire risk probability in areas of interest. The above requirements turn into EO sensors specifications. With reference to spectral bands, in order to evaluate surface and fire temperature and characteristics both of active fire and burnt surface, the Thermal InfraRed (ThIR) band and the NIR one are to be preferred because the feature of interest are dominant in those spectrum region and, especially for NIR band, slightly affected by fire gaseous emissions [1]. In addition, VIS and VNIR observation allow for evaluation of indicators of surface vegetation and potential fuels characteristics (Vegetation Indexes (VIs), Fuel Mosture Content (FMC), Water Index (WI), etc.) that are useful to evaluate local fire risk [2,3]. To carry out these estimations, multiple measures in distinct bands, preferably narrow, are necessary, hence multispectral and hyperspectral sensors and integrated sensor suites represent the most interesting solution [2,10]. The payload of integrated EO sensors that DISIS is setting up in the framework of the CRdC AMRA well suits the above objectives, in particular thanks to the two hyperspectral sensors.

A subset of the CRdC AMRA sensors mentioned in the previous section has been selected to be installed in the mini-UAV under development at DISIS. The objective is the realization of a compact UAV platform capable of autonomous operation in missions for fire risk monitoring. The selection was imposed by the limited volume and mass for the payload available on board. The thermal camera and the VNIR hyperspectral sensor were chosen because they are compatible with the available on-board resources, and they allow for the desired mission objectives, at least at basic level. Indeed, they offer the ability to identify hot spots and to observe equivalent radiant temperature distribution on the ground along with characterization of surface coverage thanks to the ThIR camera and VNIR hyperspectral camera, respectively.

The system has been conceived for pushbroom operation: sensor are installed on board to observe downwards along the flight nadir direction and subsequent areas along the ground track are observed thanks to platform movement. The ThIR camera is based on a two-dimensional arrays of detectors, so that various targets along the across-track direction are imaged simultaneously and at the same time a number of lines of targets equal to the number of pixel rows of the detector. Differently, as described in detail in the following, the hyperspectral sensor observe only one line of scene per acquisition since the rows of its detector, again a two-dimensional array of detectors, is exploited for spectral analysis of the scene.

Figure 1: Indigo OMEGA thermal camera.

A. Thermal Camera

The adopted ThIR camera is the Indigo Omega (now FLIR A10, after acquisition of Indigo by Flir Systems in 2004) (Fig. 1). Its spectral response lies in the far-infrared wavelength range of the spectrum, 7.5-13 μm, and it is based on an advanced detector, a microbolometer in Vanadium Oxide (VOx) technology, that does not need focal plane cooling. The latter feature turns into a great advantage for power consumption and compactness, which are definitely outstanding for this instrument (see 1).

Table 1. Thermal camera main specifications [11].

Detector	Uncooled microbolometer Vanadium Oxide (VOx) technology
Spectral response band	7.5 – 13 μm
Resolution	160 x 120 pixels
Noise Equivalent Temperature difference (NedT)	< 80 mK
Frame rate	Up to 25 Hz
Calibration source	Internal
Thermal stabilisation	Not needed
Cooling	Conduction to camera bottom
FOV / IFOV	40 x 30 deg / square, 0.27 deg (11mm focal length)
Output	Analog, standard PAL
Operating conditions	0 – 40 °C, umidity up to 95%
Power consumption	< 1.5 W
Mass	≤ 120 g
Dimensions	35 x 37 x 50+30 mm (camera body+lens)

Omega resolution is 160x120 pixels. The camera has an internal reference for compensation of non-uniform detector sensitivity (flat-field correction without temperature reference). The output signal is a standard analog black&white (b/w) PAL video generating 25 frames per second. Camera remote control is possible via a dedicated RS-232 I/O channel allowing for command input (on/off of auto-adjust function of brightness and contrast, selection of one of two temperature ranges –up to 150°C and up to 500°C-, flat field correction update, output image freezing, output of reference images) and reading of camera status (camera internal temperature, general settings, link test).

B. VNIR Hyperspectral Sensor

The hyperspectral system configuration envisages coupling a b/w camera equipped with a two-dimensional detector to an imaging spectrograph, the ImSpector by Specim [12]. This produces an instrument capable of observing a one-dimensional scene and of analysing the spectrum of the collected energy form each resolution element of the scene in a single acquisition. Conventional spectrometers measure the spectrum of the radiance acquired from a single scene element,

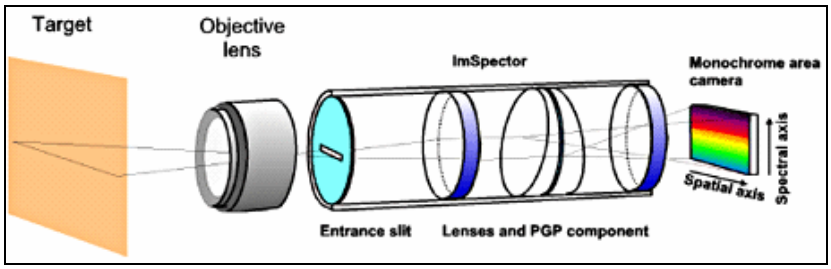

Figure 2. Imspector spectrograph functional scheme (from [12]).

Table 2. Hyperspectral sensor components main spectral specifications.

Imaging spectrograph	Model		Specim ImSpector V9
	Spectral response Band (nm)		430 – 900
	Spectral Resolution (nm)		2.7
	Number of bands		175
	Slit size (μm)		9900 x 25
	Focal plane image size (μm)		9900 x 4350
B/w camera	Model	Camera	Sony XC-ST70/CE
		Detector	Sony ICX 423 AL
	Spectral response Band (nm)		400 – 1000
	Pixel size (μm)		11.6 x 11.2
	Number of pixels		752 x 582
	Sensing area size (μm)		8720 x 6520
Hyperspectral sensor (Spettrograph + b/w camera)	Spectral response band (nm)		430 – 900
	Spectral resolution. (nm)		2.7
	Number of bands		174
	Usable image	Size (μm / pixels)	8720 x 4350 / 752 x 390
		Total pixels	2.93×10^5
	Number of required samples	Spatial x spectral	752 x 195
		Total pixels	1.47×10^5

Table 3. Hyperspectral system main specifications.

Detector	CCD
Frame rate	Up to 25 Hz
Electronic shutter	1/120 – 1/10000 s
Focal length	4.8 mm
FOV / IFOV	85° x 0.30° / 0.14° x 0.30°
Output	Analog: standard PAL
Operating conditions temperature/humudity	-5 - +45 °C / up to 95%
Power consumption	2.1 W
Mass (including ImSpector & lens)	590 g
Dimensions (including ImSpector & lens)	44 x 29 x 65 + 176 mm (camera body + ImSpector&lens)

Figure 3. Laboratory facility for calibration of the VNIR hyperspectral sensor.

scanning the spectrum in narrow wavelength bands if based on one detector or acquiring all the spectral components at the same time if using a one-dimensional array of detectors. Then, acquisition of extended scenes requires mechanical scanning. Differently, in this case the imaging spectrograph captures a line image and disperses it to its spectrum in the direction perpendicular to the line image (Fig. 2). Hence, it converts a matrix camera to a one-dimensional, spectral imaging system. The rows of each acquired frame contain images of the same line of targets but at different wavelengths. As a result, a high number of close spectral samples is acquired, producing a hyperspectral sensor. The size of the imaged scene is determined by the width of the entrance aperture of the spectrograph, a narrow slit, and by the shortest one between the length of the slit and camera detector row. The patented dispersion technique implemented in Specim Imspector operates axially, so that aberrations reduce to the utmost. It is based on a gelatinous component, resulting in a compact and light-weight sealed unit tolerating high temperature, humidity, physical shock and vibrations [12]. It is a passive component that does not require electrical power to operate. A standard objective is installed at the ImSpector entrance aperture to manage FOV size and focus.

Main specifications of the adopted components, ImSpector and b/w camera, are in 2. The same table and table 3 report the features resulting for the assembled hyperspectral systems. The camera is a COTS b/w device with standard PAL analog output and shutter time adjustable by means of dip switches on camera rear panel. The only remote control usable is a TTL trigger signal to control single image acquisition.

Activities related to this instrument have dealt with its characterization, i.e., imaging performance assessment and calibration. A specific laboratory facility has been arranged to this purpose, in which the sensor is installed on

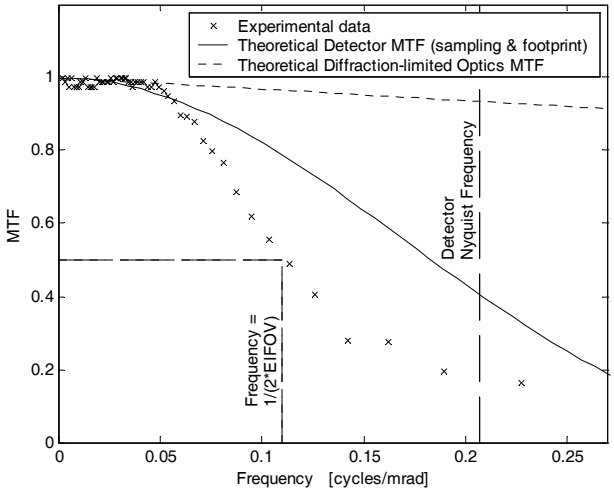

Figure 4. Experimental MTF of the hyperspectral VNIR sensor

an optical bench and test scenes are supplied to it by displaying them on a LCD computer screen (Fig. 3). Accurate relative positioning of the sensors with respect to the reference scene, i.e., the LCD screen, is operated via optical table accessories for translation and rotation. The whole facility is based on COTS components.

1. Imaging Performance

To assess imaging performance, the sensor Modulation Transfer Function (MTF), i.e., the system response to sinusoidal input radiance, has been evaluated along the spatial axis. It has been computed experimentally in the laboratory test facility following the procedure described by Boreman [13] that is based on the direct measurement of the system Contrast Transfer Function (CTF), the response to square wave input radiance. The MTF was computed as:

$$\mathrm{MTF}(\xi) = \frac{\pi}{4}\left\{\mathrm{CTF}(\xi) + \frac{\mathrm{CTF}(3\xi)}{3} - \frac{\mathrm{CTF}(5\xi)}{5} + \ldots\right\} \tag{1}$$

where ξ is the spatial frequency of the input radiance. The input square wave radiance was supplied to the sensor by showing black-and-white bar patterns with different periods on the LCD display. Figure 4 shows the obtained MTF at the imaged maximum emission wavelength (~540 nm). The Effective IFOV (EIFOV) was evaluated on the basis of the frequency $\xi_{1/2}$ at which the MTF drops to 50% of its maximum value as [15]:

$$\mathrm{EIFOV} = \frac{1}{2\,\xi_{1/2}} \tag{2}$$

Since it is $\xi_{1/2}$ =0.11 cycles/mrad (Fig. 4), the EIFOV results to be 4.54 mrad = 0.26°, while the IFOV is equal to 2.42 mrad = 0.14° for the considered sensor configuration.

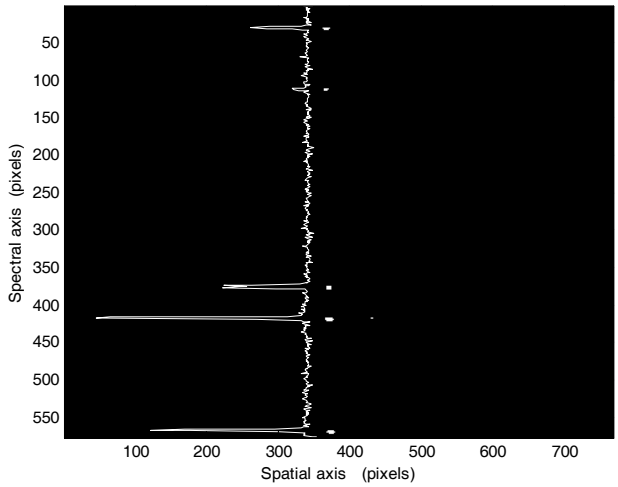

Figure 5. VNIR hyperspectral sensor output image when observing the Lot Oriel Hg(Ar) reference source (superimposed pixel intensity profile).

The same test facility has been exploited to assess sensor resolution by displaying pairs of 1-pixel-thick lines at various separations along the direction of the spatial axis of the sensor. This could be done because 1-pixel separation corresponds to about 1/5 of IFOV of the sensor in the arranged test bed. Sensor output images have been resampled in along the spatial axis direction and, then, examined accurately. A resolution of 5.3 mrad = 0.30° has been estimated, being this one the minimum separation between lines in the reference scene that appear distinct in all of the output bands according the criterion of 3-dB drop of the instrument response [15]. However, closer line pairs can still be distinguished but: i) only in part of the sensor output spectral bands; ii) until the separation is not smaller than 2.3 mrad = 0.15°.

When considering these results, worse than those expected for a classical EO device consisting of diffraction-limited optics & detector, one must be

aware that the present system includes an additional component, the spectrograph ImSpector. Also, the kind of reference scene must be taken into account.

2. Spectral calibration

The spectral axis of the detector needs calibration, i.e., determination of the function that maps output image line indexes to frequencies. It must determined experimentally and it was done by observing light sources with known emission spectrum. Line-spectrum mercury-argon Hg(Ar) lamps were adopted. Both calibration sources by Oriel and commercial lamps by Philips were used, obtaining comparable results. When imaging such a kind of light sources, single lines in the spectral direction were produced on the focal plane (Fig. 5). The calibration function (Fig. 6) was obtained after linear least-square fit of experimental data:

$$\lambda(i_{row}) = -0.782\ \ i_{row} + 874 \tag{3}$$

where $\lambda(i_{row})$ is the wavelength of the spectral band imaged on the detector line number i_{row}. The 576 lines available in the output image determine that the experimental spectral response band of the system is 424 to 873 nm.

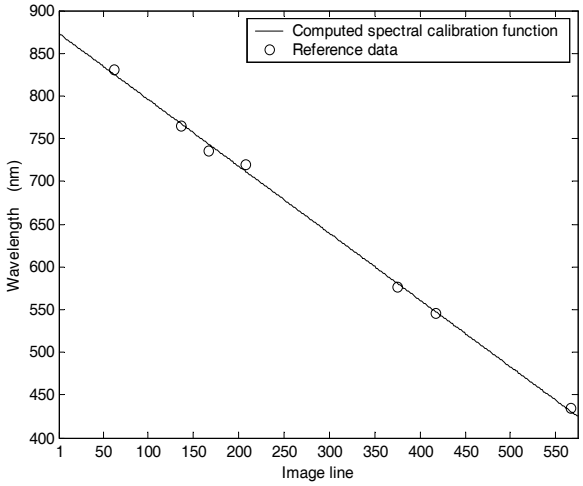

Figure 6. VNIR hyperspectral sensor spectral calibration function (reference data from several lamps).

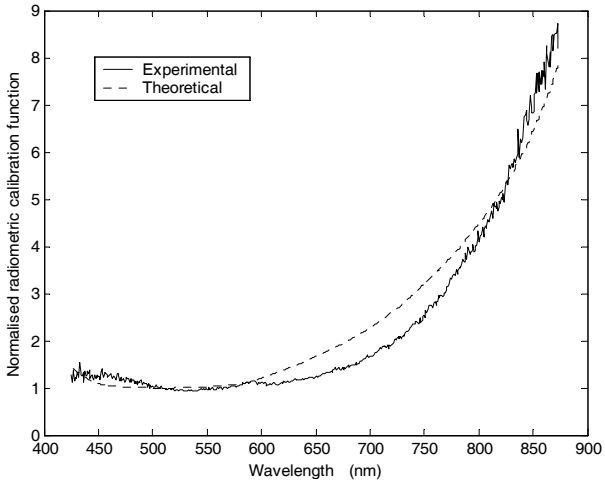

Figure 7. VNIR hyperspectral sensor radiometric calibration function.

3. Radiometric calibration

Finally, relative radiometric calibration was carried out to produce the function that compensates for non-uniform sensitivity at different wavelengths. It was generated by observing a light source with known spectral emission and comparing the output spectral profile to the input one. The corresponding ratio is the searched function. Since neither the absolute radiance emitted by the lamp toward the sensor nor the collected one could be determined, only the relative radiometric calibration function $F_{cal\,r\,r}$ has been computed, i.e., it has been normalized by referring it to the (unknown) radiance level at the first spectral interval that is observed:

$$F_{cal\,r\,r}(i_{row}) = \frac{L(i_{row})/L(i_{row0})}{V_{pix}(i_{row})/V_{pix}(i_{row0})} \tag{4}$$

where i_{row0} is the line index of the first spectral band, $L(i_{irow})$ is the reference radiance in the sensor spectral band no. i_{row} and $V_{pix}(i_{row})$ is the intensity of pixel no. i_{row}. In this case, a tungsten filament lamp was used as reference source and it was modeled as a black body radiator. Figure 7 plots the computed spectral calibration function compared to the reciprocal of the detector spectral response [16].

III. Platform and Auxiliary Systems

A. Mini-UAV Platform

The mini-UAV under development at DISIS is based on a RC-model, a reproduction of the Dornier DO27 by VMAR (Fig. 8). Its wingspan is 2.75m and its length is 1.7m. It is equipped with a 28cc engine. It offers wide, regular volumes in the front and central part of the fuselage for installing avionics and payload. Currently, the avionics system installed for navigation experiments consists of an INS/GPS integrated system [14]. It includes an embedded computer (a Pentium-based pc104 unit by Ampro running the real-time operating system WxWorks) that gathers and processes the output of a strapdown inertial measurement unit by Crossbow, and a GPS receiver by Trimble. The navigation functionalities are of great importance because they allow for spatial referentiation of the observed scene.

Figure 8. DISIS mini-UAV aircraft.

B. On-Board Auxiliary Sub-Systems of the Payload

The core of the RS payload is represented by the two EO sensors described in the previous section. It also includes a computer for operation management and a radio communication system for data downlink and command uplink. Their main characteristics are in table 4.

The task of the on-board computer is control of sensor operation, storage and real-time elaboration of remotely sensed data, and management of communications with the ground station. A pc104 unit has been selected and it has been equipped with a frame grabber to acquire the output of the two sensor, a power conditioning unit to generate stable electrical voltage for cameras and transceiver, and a power relay module to switch payload units on or off as needed for minimum power consumption. (Fig. 9).

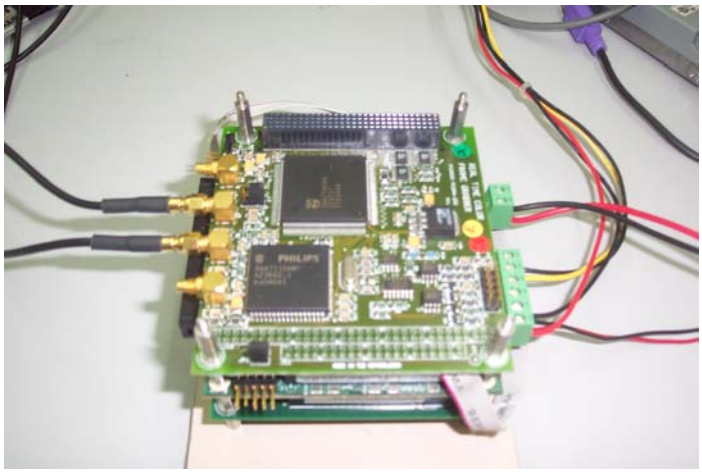

Figure 9. Payload-dedicated on-board computer.

With reference to communications, a digital link has been envisaged because:

– it can be efficiently integrated both on board and at the ground station, since at both

Table 4. main characteristics of the on-board auxiliary subsystems.

	DISIS mini-UAV mission
CPU	AMPRO pc104 format, 400MHz Celeron, 256MB RAM, RS-232/422/485, LAN, and USB1.1 ports, compact flash + 2.5" hhd
Frame grabber(s)	- 4-ch (mux) analog frame grabber
Power	< 15 W
Mass	< 0.2 kg
RF communication	Aerocomm AC 5124 transceiver
Frequency	77 non-interfering channels in 2.402 – 2.478 GHz
Transmission technique	FHSS
Transmitted power	200 mW
RF data rate	Up to 882 kbps
Sensitivity	-90 dBm
Operating conditions	-40 - +80°C / < 90% humidity (non condensing)
Power consumption	0.95 / 1.4 / 2.4 W (25% / 50% / 100% Tx) 0.55 W (100%Rx) / 0.22 W (interface On, RF Off)
Mass	< 20 g
Dimensions	42 x 68 x 5 mm

locations digital CPUs are in use;
- it offers great flexibility in managing different kind of data;
- there exist COTS systems which can be adopted without need of customization.

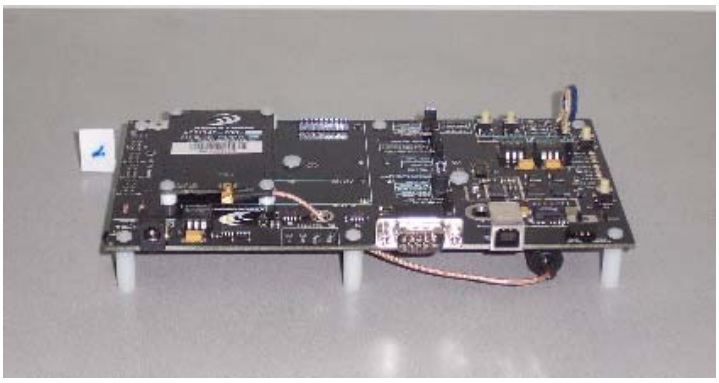

Figure 10. AC-5124 developer kit and transceiver.

After a preliminary analysis of typical operating conditions, it has resulted that the cameras output flows at high data rate from tens of kB/s to tens of MB/s. Hence, to guarantee adequate real-time downlink capability, attention has been focused on existing COTS systems capable high data rate and compatible with installation on compact mobile platforms. The search was carried out among products available on the market during year 2004. Two different solutions were identified: radio-modem transceivers, operating up 880kbps, and PC radiolan devices, capable of more than 10Mbps. The former ones have been preferred because can guarantee link operating ranges in the order of thousand meters, whilst compact radiolan mobile units performance is at least one order of magnitude lower. The requirement on link operation range has been considered definitely dominant with respect to maximum data rate. When full data stream is larger than channel capacity, partial download is adopted and data are pre-processed on board. Solutions can be represented by image resolution degradation or data compression.

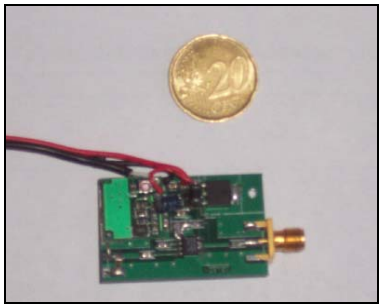

Figure 11. Analog video signal transmitter.

The selected device is the AC5124 transceiver by Aerocomm (Fig. 10). It operates at 2.4 GHz and adopts the Frequency Hopping Spread Spectrum (FHSS) transmission technique [17], which allows for RF data rate up to 882kbps and line-of-sight operational range in the order of 3.5 km with 200 mW transmitted power. The device can be easily connected to a CPU via standard pc ports thanks to its TTL serial interface. The Developer Kit optional unit supplies serial RS-232, RS-422, and USB standard connections. Further features of the system are in table 4. Two identical units are used, one connected to the on-board CPU and one to the ground station computer.

Also an analog video transmitter (200mW at 2.4 GHz) has been envisaged, to be used as an alternative to the digital channel. It is particularly interesting for its compactness (38x20x5 mm, Fig. 11) and low power consumption (<2W).

C. Ground Station

The ground station is being developed with specific reference to the tasks of the digital communication system ground terminal. It consists of a transportable, high performance personal computer connected to the ground transceiver. RS-232, RS-422/485, and USB ports are available. The unit is also equipped with interfaces to acquire the output of generic EO sensors, i.e., a Camera Link frame grabber and a four-channel analog one, making tests of any payload unit possible before flight. Also two IEEE 1394 firewire ports are available.

It is worth noting that the presence of the analog frame grabber allows this system to be used as ground station also for the analog transmission system. In fact, in this case the analog video signal demodulated by the radio-receiver can be acquired via the analog frame grabber and, then, digitalized, stored, and processed.

Maintenance-free batteries were chosen as power source for use during outdoor test campaigns. Two 12-Vdc, 40-Ah units are connected in series to supply the CPU with the required 24-Vdc power. Lower voltages are derived by means of dc-dc converters to power radio receivers and other devices. Gel-electrolyte-based batteries were selected because offering trouble-free transportation. Considering worst-case overall power consumption of 500W (20.8A at 24 Vdc), autonomy of nearly 2 hours is guaranteed.

IV. Conclusion

A modern multi-band/hyper-spectral payload of electro-optical sensors has been presented in this paper. Its has been conceived to be operated from a UAV in missions aimed at natural disasters monitoring, in particular forest fires. The core of the payload, described in detail in the paper, is an integrated sensor including a thermal imager and a VNIR hyperspectral camera. Analysis of sensors performance and configuration of the payload have been described, including its CPU and communications subsystems.

Acknowledgments

The activities described above are being carried out under the sponsorship of "Centro Regionale di Competenza Analisi e Monitoraggio del Rischio Ambientale", that supported the acquisition of the electro-optical sensors, of Regione Campania, that supported the development of the digital communication system for an unmanned platform, and of the Ministry of Education, University and Research. All of the projects are co-funded by the Department of Space Science and Engineering of the University of Naples "Federico II".

References

[1]P.J. Riggan, J.W. Hoffman, and J.A. Brass, "Estimating Fire Properties by Remote Sensing," *Proc. of IEEE Aerospace Conference 2000*, Big Sky, USA, pp. 173-179.

[2]D. A. Roberts and P. E. Dennison, "Hyperspectral technologies for wildfire fuel mapping," *Proc. 4th Int. Worshop Rem. Sens. & GIS to Forest Fire Management*, 2003, 10 pp.

[3]J. Verbesselt, S. Fleck, and P. Coppin, "Estimation of fuel moisture content towards Fire Risk Assessment: A review," in *Forest Fire Research & Wildland Fire Safety* edited by Viegas, Millpress, Rotterdam (The Netherlands), 2002, 11 pp.

[4]N. El-Sheimy and B. Wright, "Real-time Airborne Mapping System for Forest Fire Fighting (F3) System," *PERS*, Vol. 70, No. 4, 2004, pp.381-383.

[5]V.G. Ambrosia, S.S. Wegener, D.V. Sullivan, S.W. Buechel, S.E. Dunagan, J.A. Brass, J. Stoneburner, and S, M. Schoenung, "Demonstrating UAV-Acquired Real-Time Thermal Data over Fires," *PERS*, Vol. 69, No. 4, 2004, pp. 391-402

[6]J.A. Brass, V.G. Ambrosia, R.S. Dann, R.G. Higgins, E.A. Hildum, J. McIntire, P.J. Riggan, S.M. Schoenung, R.E. Slye, D.V. Sullivan, S. Tolley, R.Vogler, S.S. Wegener, "First Response Experiment (FiRE) Using An Uninhabited Aerial Vehicle (UAV)," *Proc. of Fifth International Airborne Remote Sensing Conference, San Francisco, 17-20 September*, 2001, 9 pp.

[7]J.A. Brass, V. Ambrosia, J.D, Ricker jr., and A.C. Roberts, "Forest Firefighting from Real-Time Airborne Infrared Remote Sensing," *Proc. of Fifth International Airborne Remote Sensing Conference, San Francisco, 17-20 September*, 2001, pp 21.

[8]A. Barducci, D. Guzzi, P. Marcoionni, and I. Pippi, "Infrared detection of active fires and burnt areas: theory and observations," *Infrared Physics & Technology*, Vol. 43, 2002, pp. 119-125.

[9]G. Rufino and A. Moccia, "UAV Remote Sensing Payload for Natural Disasters Monitoring," *Proc. 28th Conference of the Italian Association of Aeronautics and Astronautics*, Volterra (Italy), 19-22 September, 2005, 10 pp.

[10]P. Shippert,"Why Use Hyperspectral Imagery," *PERS*, Vol. 70, No. 4, 2004, pp. 377-380.

[11]Indigo system Corporation, "Omega Camera User Manual," doc. no. 412-0006-10, v. 110, 2002.

[12]Specim, *ImSpector user manual*, v. 2.21, 2003.

[13]G.D. Boreman, Modulation Transfer Function In Optical and Electro-Optical Systems, SPIE Press, Bellingham, USA, 2001.

[14]D. Accardo, F. Esposito, and A. Moccia, "Low-cost Avionics for Autonomous Navigation Software/Hardware Testing," Proc. IEEE Aeroconf 2004, Vol. 5, 2004, pp. 3016-3024.

[15]G.C. Holst, *Electro-Optical Imaging System Performance*, SPIE Press, Bellingham, USA, 2000.

[16]Sony Corporation, "XC-ST70/70CE User's Guide,", v. 1.0, 1999.

[17]Aerocomm inc., AC5124 2.4 GHz OEM Transceiver User Manual,, v. 4.4, 2003.